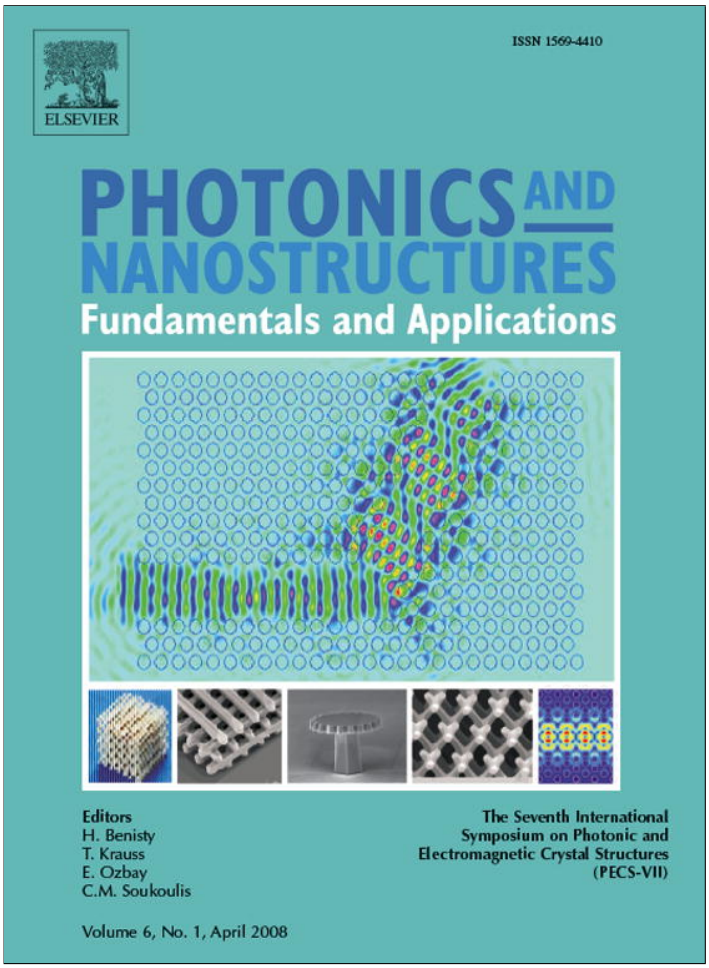

Available online at www.sciencedirect.com
ScienceDirect
ELSEVIER
Photonics and Nanostructures – Fundamentals and Applications 6 (2008) 87–95
PHOTONICS AND NANOSTRUCTURES Fundamentals and Applications
www.elsevier.com/locate/photonics

Design of electromagnetic cloaks and concentrators using form-invariant coordinate transformations of Maxwell's equations

Marco Rahm [a,*], David Schurig [a], Daniel A. Roberts [a], Steven A. Cummer [a], David R. Smith [a], John B. Pendry [b]

[a] *Department of Electrical and Computer Engineering, Duke University, Box 90291, Durham, NC 27708, USA*
[b] *Department of Physics, The Blackett Laboratory, Imperial College, London SW7 2AZ, UK*

Received 15 June 2007; accepted 30 July 2007
Available online 8 August 2007

Abstract

The technique of applying form-invariant, spatial coordinate transformations of Maxwell's equations can facilitate the design of structures with unique electromagnetic or optical functionality. Here, we illustrate the transformation-optical approach in the designs of a square electromagnetic cloak and an omni-directional electromagnetic field concentrator. The transformation equations are described and the functionality of the devices is numerically confirmed by two-dimensional finite element simulations. The two devices presented demonstrate that the transformation optic approach leads to the specification of complex, anisotropic and inhomogeneous materials with well directed and distinct electromagnetic behavior.

PACS : 42.15.Eq; 42.25. −p; 42.25.Bs; 42.25.Fx; 02.40. −k; 02.70.Dh; 04.30.Nk

Keywords: Transformation optical design; Form-invariant coordinate transformations of Maxwell's equations; Electromagnetic theory; Metamaterials; Cloaking; Anisotropic media; Inhomogeneous media; Numerical full-wave simulations; Finite-element method

1. Introduction

In a theoretical study, Pendry et al. reported a general method for the design of electromagnetic materials based on form-invariant transformations of Maxwell's equations [1]. In that paper, the methodology of transformation optics was applied to find the specification for an electromagnetic cloak-a complex material capable of rendering objects within its interior invisible to detection. Although just one example of the many intriguing structures possible using the transformation optical approach, the proposed cloak design generated enormous interest in its own right. An approximation to the invisibility cloak based on metamaterials was subsequently realized by Schurig et al., who demonstrated the cloaking mechanism in microwave experiments [2]. The transformation optical approach to invisibility is quite general, differing in scope from prior related work. Indeed, methods of reducing the electromagnetic scattering of objects at radar frequencies have long been a subject of intense research [3–5]. On the nanoscale, techniques have also been suggested to reduce the scattering of one or more multipole components of size-limited objects using tailored negative index or negative permittivity coatings [6,7]. More recently, a mathematically rigorous proof of an

* Corresponding author. Tel.: +1 919 660 8259.
E-mail address: marco.rahm@duke.edu (M. Rahm).

1569-4410/$ – see front matter
doi:10.1016/j.photonics.2007.07.013

invisibility structure based on active devices was reported [8].

Transformation optics provides for a conceptually simple approach to the design of complex electromagnetic structures: one imagines warping space to achieve the desired electromagnetic functionality. The trajectories of electromagnetic waves passing through a region of warped space must conform to the local metric, and this provides an alternative (though conceptual) means to control and manipulate electromagnetic fields. Once the desired design is determined, the coordinate transformation and its Jacobi matrix determine the transformation of Maxwell's equations and the constitutive relations. The result provides the specification for an electromagnetic structure that is complex-being inhomogeneous and anisotropic-but realizable for example through artificially structured metamaterials. Indeed, because the fields in a volume bounding a transformation optical structure are identical to those that would exist where the structure is replaced by free space, anisotropy is necessary to circumvent uniqueness constraints [8].

If the coordinate transformation can be realized exactly in the constitutive parameters, all aspects of wave propagation will be transformed by the structure, including the near-fields. Adding constraints to the materials reduces the ultimate performance of the structure, but nevertheless can still allow for interesting and novel structures. Leonhardt, for example, has shown that if the materials are restricted to be isotropic, an approximate cloak can be constructed that is valid in the geometrical optic limit [9]. Likewise, constraints were employed for the metamaterial cloak utilized by Schurig et al. to ease the metamaterial design and fabrication, resulting in a structure that produced significant reflection yet still demonstrated the cloaking mechanism for transmitted waves [2].

Since the concept of transformation optics was introduced, there have been a growing number of subsequent reports applying the method to a variety of electromagnetic, acoustic and elasto-mechanical structures [10–17]. Full wave simulations have helped to confirm the expected behavior and have provided a platform to explore systematically the effects of absorption, imperfections and other constraints that are inherent to fabricated realizations of the transformation optical structures [18,19].

In this paper we present two examples that demonstrate the general applicability of form-invariant coordinate transformations for the design of complex, inhomogeneous and anisotropic electromagnetic materials with well-defined functionality. For the first example, we derive the electromagnetic constitutive parameters corresponding to a two-dimensional electromagnetic cloak having square cross-section. The square shape has been chosen to illustrate the nature of the transformation and the resulting design for a structure that lacks rotational symmetry in the plane. In contrast to the cylindrical cloaks with circular cross-section previously presented, the square cloak design results in a non-orthogonal transformation producing a more complicated specification for the spatially dependent permittivity and permeability tensors. The method to design this structure, however, can be applied to the design of structures with arbitrary shape.

For the second example, we derive the material properties of an electromagnetic field concentrator by the same approach. The purpose of the cylindrical concentrator is to focus incident electromagnetic waves with wave vectors perpendicular to the cylinder axis, enhancing the electromagnetic energy density of incident waves in a given area. This example illustrates the strength of the transformation-optical approach for designing devices other than cloaks.

2. Transformation equations

In this section, the formulas describing the spatial coordinate transformations and the calculation of the resulting material parameters, i.e. the electric permittivity tensor and the magnetic permeability tensor, are derived. The methodology used to compute the electromagnetic material properties is similar to the one reported in [20].

For convenience, we denote Maxwell's equations in the Minkowski form [21]

$$\partial_{[\kappa}F_{\lambda\nu]} = 0 \tag{1}$$

$$\partial_{\nu}G^{\nu\lambda} = j^{\lambda}, \quad \kappa,\lambda,\nu = 0,1,2,3 \tag{2}$$

where the square brackets express an alternation among the indices [22] and the skew-symmetric covariant and contravariant tensors $F_{\lambda\nu}$ and $G^{\nu\lambda}$ and the contravariant vector j^{λ} possess the identifications

$$F_{\lambda\nu} = \begin{pmatrix} 0 & -E_1 & -E_2 & -E_3 \\ E_1 & 0 & B_3 & -B_2 \\ E_2 & -B_3 & 0 & B_1 \\ E_3 & B_2 & -B_1 & 0 \end{pmatrix} \tag{3}$$

$$G^{\nu\lambda} = \begin{pmatrix} 0 & D_1 & D_2 & D_3 \\ -D_1 & 0 & H_3 & -H_2 \\ -D_2 & -H_3 & 0 & H_1 \\ -D_3 & H_2 & -H_1 & 0 \end{pmatrix} \tag{4}$$

$$j^{\lambda} = \begin{pmatrix} \rho \\ j_1 \\ j_2 \\ j_3 \end{pmatrix} \tag{5}$$

where E is the electric field, B is the magnetic induction, D is the electric displacement, H is the magnetic field, ρ is the volume charge density, j is the current density and the indices denote their spatial components. In this notation, the coordinate vector in four-space is $x^{\alpha} = (x_0 = t, x_1, x_2, x_3)^T$ with the vacuum speed of light c set to unity.

For a linear medium, the constitutive relation can be written as

$$G^{\lambda\nu} = \frac{1}{2}\chi^{\lambda\nu\sigma\kappa}F_{\sigma\kappa} \tag{6}$$

where the tensor $\chi^{\lambda\nu\sigma\kappa}$ contains the complete information about the electromagnetic material properties.

The Minkowski Eqs. (1) and (2) and the constitutive relation (6) are form-invariant for arbitrary continuous space-time transformations of the form

$$x^{\alpha'}(x^{\alpha}) = A^{\alpha'}_{\alpha}x^{\alpha} \tag{7}$$

where $A^{\alpha'}_{\alpha} = \frac{\partial x^{\alpha'}}{\partial x^{\alpha}}$ are the elements of the Jacobian transformation matrix and the primed indices denote the space-time coordinates of the vector x in the transformed space.

Considering the transformation (7), the Minkowski Eqs. (1) and (2) transform as

$$\partial_{[\kappa'}F_{\lambda'\nu']} = A^{\kappa}_{\kappa'}A^{\lambda}_{\lambda'}A^{\nu}_{\nu'}\partial_{[\kappa}F_{\lambda\nu]} = 0 \tag{8}$$

$$\partial_{\nu'}G^{\nu'\lambda'} = \left[\det(A^{\lambda'}_{\lambda})\right]^{-1}A^{\lambda'}_{\lambda}\partial_{\nu}G^{\nu\lambda}$$

$$\partial_{\nu'}G^{\nu'\lambda'} = \left[\det(A^{\lambda'}_{\lambda})\right]^{-1}A^{\lambda'}_{\lambda}j^{\lambda} \tag{9}$$

$$\partial_{\nu'}G^{\nu'\lambda'} = j^{\lambda'} \tag{10}$$

and the constitutive relation transforms as

$$\begin{aligned} G^{\lambda'\nu'} &= \left[\det(A^{\lambda'}_{\lambda})\right]^{-1}A^{\lambda'}_{\lambda}A^{\nu'}_{\nu}G^{\lambda\nu} \\ &= \frac{1}{2}\left[\det(A^{\lambda'}_{\lambda})\right]^{-1}A^{\lambda'}_{\lambda}A^{\nu'}_{\nu}A^{\sigma'}_{\sigma}A^{\sigma}_{\sigma'}A^{\kappa'}_{\kappa}A^{\kappa}_{\kappa'}\chi^{\lambda\nu\sigma\kappa}F_{\sigma\kappa} \\ &= \frac{1}{2}\left[\det(A^{\lambda'}_{\lambda})\right]^{-1}A^{\lambda'}_{\lambda}A^{\nu'}_{\nu}A^{\sigma'}_{\sigma}A^{\kappa'}_{\kappa}\chi^{\lambda\nu\sigma\kappa}A^{\sigma}_{\sigma'}A^{\kappa}_{\kappa'}F_{\sigma\kappa} \\ &= \frac{1}{2}\chi^{\lambda'\nu'\sigma'\kappa'}F_{\sigma'\kappa'} \end{aligned} \tag{11}$$

with

$$\chi^{\lambda'\nu'\sigma'\kappa'} = \left[\det(A^{\lambda'}_{\lambda})\right]^{-1}A^{\lambda'}_{\lambda}A^{\nu'}_{\nu}A^{\sigma'}_{\sigma}A^{\kappa'}_{\kappa}\chi^{\lambda\nu\sigma\kappa} \tag{12}$$

$$F_{\sigma'\kappa'} = A^{\sigma}_{\sigma'}A^{\kappa}_{\kappa'}F_{\sigma\kappa} \tag{13}$$

where $\det(X)$ indicates the determinant of a tensor X.

It is obvious, that the form-invariance of the Minkowski Eqs. (1) and (2) and the constitutive relation (6) also hold for transformations which only address the space coordinates, as the space manifold is a submanifold of the space-time manifold. In the following we will restrict ourselves to time-independent, spatial coordinate transformations. Under this restriction, the constitutive parameters, i.e. the tensors of the permittivity and the permeability of a linear, anisotropic, non-dispersive, non-bianisotropic and locally interacting medium can be written in a more accessible form as

$$\epsilon^{i'j'} = \left[\det(A^{i'}_{i})\right]^{-1}A^{i'}_{i}A^{j'}_{j}\epsilon^{ij} \tag{14}$$

$$\mu^{i'j'} = \left[\det(A^{i'}_{i})\right]^{-1}A^{i'}_{i}A^{j'}_{j}\mu^{ij} \tag{15}$$

The relations (7), (14) and (15) form the underlying equations for the calculation of the electromagnetic material parameters used in the design of a square-shaped cloak and a concentrator for electromagnetic fields.

For all the transformations considered in the next sections, the mathematical starting point is three-dimensional, euclidian space expressed in a cartesian coordinate system $x^i = (x_1, x_2, x_3)^T$. From the physical point of view, the space is considered to be medium-free (vacuum) and isotropic. Thus, the permittivity tensor ϵ^{ij} and the permeability tensor μ^{ij} of the original space can be expressed in the form

$$\epsilon^{ij} = \varepsilon_0\delta^{ij} \tag{16}$$

$$\mu^{ij} = \mu_0\delta^{ij} \tag{17}$$

with $(\delta^{ij} = 1)$ for $(i = j)$ and $(\delta^{ij} = 0)$ elsewhere.

2.1. Square cloak

The coordinate transformation equations for the electromagnetic design of a square-shaped cloak with a sidelength $2s_1$ of the inner square and a sidelength $2s_2$ of the outer square (see Fig. 1a) are expressed by

$$x'_1(x_1, x_2, x_3) = x_1\frac{s_2 - s_1}{s_2} + s_1 \tag{18}$$

$$x'_2(x_1, x_2, x_3) = x_2\left(\frac{s_2 - s_1}{s_2} + \frac{s_1}{x_1}\right) \tag{19}$$

$$x'_3(x_1, x_2, x_3) = x_3 \tag{20}$$

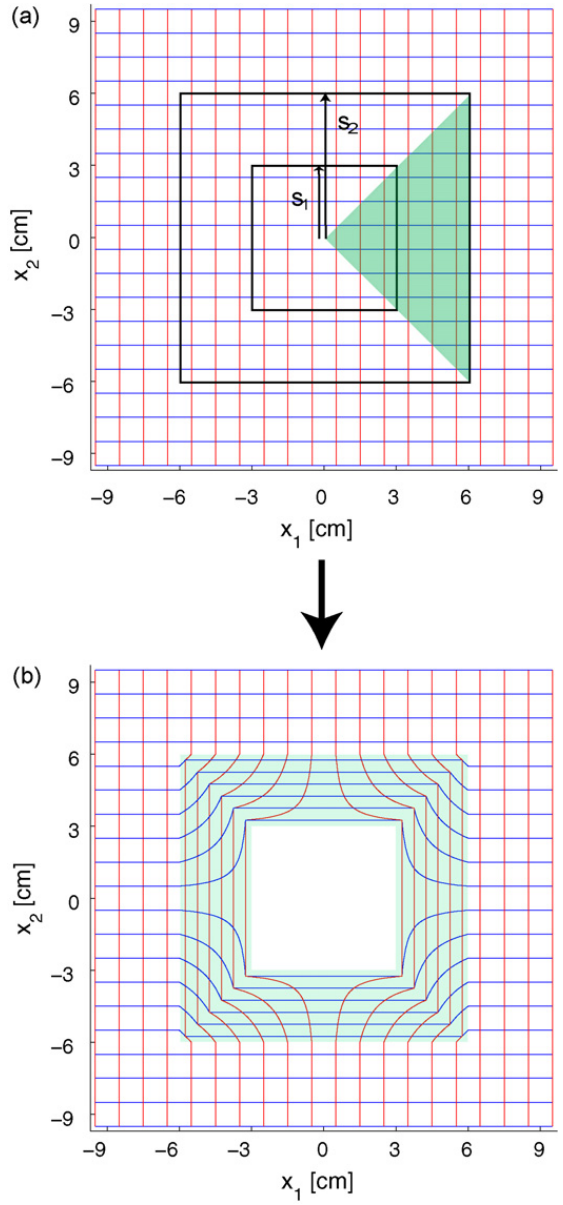

Fig. 1. Spatial coordinate transformation for the design of a square-shaped cloak (a) original space, s_1: half sidelength of the inner square, s_2: half sidelength of the outer square. The transformation Eqs. (18)–(20) are only valid in the green shadowed region (b) transformed space.

with the Jacobi matrix and its determinant

$$A_i^{i'} = \begin{pmatrix} \frac{s_2 - s_1}{s_2} & 0 & 0 \\ \frac{-x_2}{x_1^2} s_1 & \frac{s_2 - s_1}{s_2} + \frac{s_1}{x_1} & 0 \\ 0 & 0 & 1 \end{pmatrix} \tag{21}$$

$$\det(A_i^{i'}) = \frac{s_2 - s_1}{s_2} \left(\frac{s_2 - s_1}{s_2} + \frac{s_1}{x_1} \right) \tag{22}$$

for $(0 < x_1 \leq s_2)$, $(-s_2 < x_2 \leq s_2)$, $|x_2| < |x_1|$ and $(|x_3| < \infty)$. It should be noted, that, by the foregoing definitions, the transformation Eqs. (18)–(20) are only defined for the green shadowed area in Fig. 1a and that the transformation is continuous at the boundary of the transformed domain. The corresponding transformation formulas for the upper, left, and lower domain of the square cloak can be readily obtained by applying rotation operators with rotation angles of $\pi/2$, π and $3\pi/2$ around the z-axis to Eqs. (18)–(20).

As can be seen from Fig. 1b, the transformation expands the space within the inner square at the expense of a compression of space between the inner and outer square. Inserting Eqs. (21) and (22), (16) and (17) into (14) and (15), applying the reverse transformations $x^i(x^{i'})$ of (18)–(20) and dividing (14) by ε_0 and (15) by μ_0 yields the relative permittivity and the relative permeability tensors $(\epsilon_r)^{i'j'}$ and $(\mu_r)^{i'j'}$, expressed in the coordinates $x^{i'}$ of the transformed space, as

$$(\epsilon_r)^{i'j'} = (\mu_r)^{i'j'} = \begin{pmatrix} \frac{c}{a} & -\frac{b}{a} & 0 \\ -\frac{b}{a} & \frac{a^2 + b^2}{ac} & 0 \\ 0 & 0 & ac \end{pmatrix} \tag{23}$$

with

$$a := \frac{s_2}{s_2 - s_1},\ b := \frac{x_2'}{(x_1')^2} a s_1,\ c := a\left(1 - \frac{s_1}{x_1'}\right) \tag{24}$$

Due to the natural invariance of the Minkowski equations (as discussed in [20]), the permittivity and permeability tensors can also be interpreted as the material properties of a medium described in the coordinate system of the original space by substituting the primed indices by unprimed indices (“material interpretation”). Again it should be noted, that the material properties (23) are only valid in the green shadowed region of Fig. 1a and that, due to the symmetry of the cloak, the material properties of the other cloak domains can be readily obtained by rotating the tensors in (23) by $\pi/2$, π and $3\pi/2$, respectively. Furthermore, the relative permittivity and permeability tensors are non-diagonal, which is a direct consequence of the non-conformality of the transformation (18)–(20). However, in terms of fabricating such a material, it is desirable to have the material parameters denoted in their eigenbasis, where the permittivity and permeability tensors are diagonal. Due to the symmetry of the tensors ϵ^{ij} and μ^{ij}, an eigenbasis solution always exists

and one obtains

$$(\epsilon_r)^{ij} = (\mu_r)^{ij} = \frac{1}{2ac}\begin{pmatrix} \left(A+\sqrt{(B)}\right) & 0 & 0 \\ 0 & \left(A-\sqrt{(B)}\right) & 0 \\ 0 & 0 & 2a^2c^2 \end{pmatrix} \tag{25}$$

with

$$A := a^2 + b^2 + c^2 \tag{26}$$

$$B := a^2(a^2 + 2(b^2 - c^2)) + b^2(b^2 + 2c^2) + c^4 \tag{27}$$

Notice, that the primes were omitted to express the electromagnetic parameters in the material interpretation. Due to the spatial dependence of the elements of the permittivity and permeability tensors, the orientation of the basis vectors (x, y) of the eigenbasis depends on the spatial location (x_1, x_2) within the cloak material. This is illustrated in Fig. 2a for a square cloak with $s_1 = 3$ cm and $s_2 = 6$ cm. The graph shows the rotation angle of the eigenbasis vectors (x, y) in dependence on the location x_1 at different positions x_2. Again, the physical quantities are calculated for the green shadowed region in Fig. 1a. The rotation angle of the eigenbasis with refer to the coordinate system (x_1, x_2) varies within a range from 1.3 to 1.8 rad. In order to fabricate such a medium as a metamaterial, the principle axes of the unit cells have to be individually aligned along the basis vectors (x, y, z) of the eigenbasis.

Fig. 2b–d shows the values of the relative permeabilities $\mu_x := \mu_r^{11}$ and $\mu_y := \mu_r^{22}$ and the relative permittivity $\epsilon_z := \epsilon_r^{33}$ in dependence on the location within the cloak. These three physical quantities deliver a full description of the propagation behavior of an electromagnetic wave with a linear polarization vector of the electric field oriented along the z-direction. The depicted area corresponds to the green shadowed region in Fig. 1a. As opposed to μ_y and ϵ_z, the value of μ_x diverges at the boundary of the inner square of the cloak. However, at a distance of about 1.6 mm from the inner boundary of the square cloak, μ_x already approaches finite values below 35 as determined along a straight intersection line parallel to the y-axis at $x = 3.16$ cm. Please note, that Fig. 2b only displays the permeability μ_x for $x \geq 3.16$ cm and thus does not show the divergence of the relative permeability towards the inner boundary of the cloak. However, assuming a typical unit cell size of 3.3 mm for a fabricated effective medium at a working frequency of 8.5 GHz, the value of μ_x at the midpoint of the unit cells at the inner boundary of the cloak is between 19 and 35, so that an implementation of such a material is still possible. Although the effective μ_x is inaccurate in the vicinity of the boundary of the inner square, it can be shown, that the performance of the implemented device is not affected by this fact, which is out of the scope of this paper.

2.2. Cylindrical concentrator

Due to its cylindrical symmetry, it is convenient to describe the transformation equations in a cylindrical coordinate system. In this context, it is necessary to consider the transformation from cartesian to cylindrical coordinates for an isotropic medium with

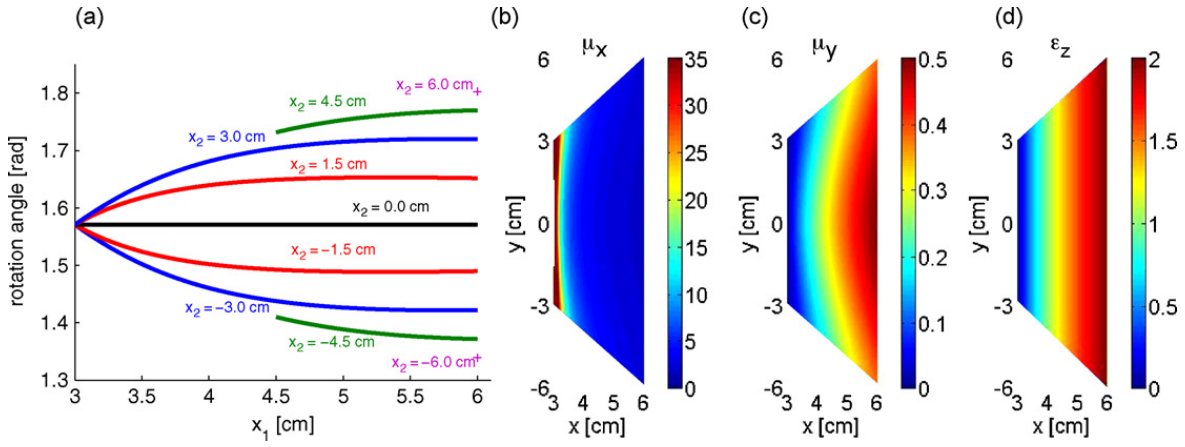

Fig. 2. (a) Rotation angle of the eigenbasis vectors (x, y) in dependence on their spatial location (x_1, x_2) within the cloaking material calculated for the green shadowed region in Fig. 1a. (b–d) Spatial dependence of the material parameters of the square cloak medium for a TE-wave polarized in z-direction, expressed in their local eigenbasis (x, y, z), (b) permeability μ_x in x-direction, (c) permeability μ_y in y-direction and (d) permittivity ϵ_z in z-direction.

permittivity ϵ and permeability μ. With the transformation

$$r'(x_1,x_2,x_3) = \sqrt{x_1^2 + x_2^2} \tag{28}$$

$$\phi'(x_1,x_2,x_3) = \arctan\left(\frac{x_2}{x_1}\right) \tag{29}$$

$$x_3'(x_1,x_2,x_3) = x_3 \tag{30}$$

and Eqs. (14) and (15) one obtains

$$\eta^{i'j'} = \begin{pmatrix} r'\eta & 0 & 0 \\ 0 & \dfrac{\eta}{r'} & 0 \\ 0 & 0 & r'\eta \end{pmatrix} \quad \text{with} \quad \eta = \epsilon, \mu \tag{31}$$

At this point, the reader should be aware, that the metric tensor of the transformed space is

$$g_{i'j'} = \begin{pmatrix} 1 & 0 & 0 \\ 0 & r'^2 & 0 \\ 0 & 0 & 1 \end{pmatrix} \tag{32}$$

so that (31) necessarily still represents the material properties of an isotropic medium.

The transformation equations for the optical design of the cylindrical concentrator are denoted as

$$r''(r',\phi',x_3') = \begin{cases} \dfrac{R_1}{R_2} r' & 0 \le r' \le R_2 \\ \dfrac{R_3 - R_1}{R_3 - R_2} r' - \dfrac{R_2 - R_1}{R_3 - R_2} R_3 & R_2 < r' \le R_3 \end{cases} \tag{33}$$

$$\phi''(r',\phi',x_3') = \phi' \quad 0 \le \phi' < 2\pi \tag{34}$$

$$x_3''(r',\phi',x_3') = x_3' \quad -\infty < x_3' < \infty \tag{35}$$

with the corresponding Jacobi tensors and determinants

$$A_i^{i'} = \begin{cases} \begin{pmatrix} \dfrac{R_1}{R_2} & 0 & 0 \\ 0 & 1 & 0 \\ 0 & 0 & 1 \end{pmatrix} & 0 \le r' \le R_2 \\ \begin{pmatrix} \dfrac{R_3 - R_1}{R_3 - R_2} & 0 & 0 \\ 0 & 1 & 0 \\ 0 & 0 & 1 \end{pmatrix} & R_2 < r' \le R_3 \end{cases} \tag{36}$$

$$\det(A_i^{i'}) = \begin{cases} \dfrac{R_1}{R_2} & 0 \le r' \le R_2 \\ \dfrac{R_3 - R_1}{R_3 - R_2} & R_2 < r' \le R_3 \end{cases} \tag{37}$$

The space transformation is visualized in Fig. 3. Space is compressed into a cylindrical region with radius R_1 at the expense of an expansion of space between R_1 and R_3. The transformation is continuous to free space at R_3. Inserting (31), (36) and (37) into (14) and (15) and renormalizing (31) by requiring ($\eta^{1'1'} \mapsto \eta^{1'1'}/(r'\eta), \eta^{2'2'} \mapsto \eta^{2'2'} r'/\eta, \eta^{3'3'} \mapsto \eta^{3'3'}/(r'\eta)$) to conveniently describe the relative material properties of free space as $\eta_r^{i'j'} = \delta^{i'j'}$ in cylindrical coordinates, one obtains with help of the inverse transformations of (33)–(35) the relative permittivity and permeability tensors, expressed in the coordinates (r'',ϕ'',z'') as

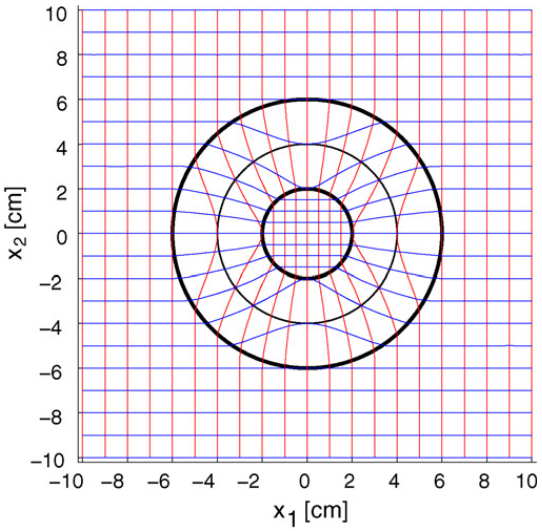

Fig. 3. Visualization of the space transformation expressed in (33)–(35). Space is compressed into a cylindrical region with radius $R_1 = 2$ cm (black inner circle) at the expense of an expansion of space between R_1 and $R_3 = 6$ cm (black outer circle). The displayed intermediate circle is located at $R_2 = 4$ cm.

$$\epsilon_r^{i''j''} = \mu_r^{i''j''} = \begin{cases} \begin{pmatrix} 1 & 0 & 0 \\ 0 & 1 & 0 \\ 0 & 0 & \left(\dfrac{R_2}{R_1}\right)^2 \end{pmatrix} & 0 \le r'' \le R_1 \\ \begin{pmatrix} \eta_r & 0 & 0 \\ 0 & (\eta_r)^{-1} & 0 \\ 0 & 0 & \left(\dfrac{f}{h}\right)^2 \eta_r \end{pmatrix} & R_1 < r'' \le R_3 \end{cases} \tag{38}$$

with

$$\eta_r = \frac{e}{f}\frac{R_3}{r''} + 1 \tag{39}$$

$$e := R_2 - R_1,\ f := R_3 - R_2,\ h := R_3 - R_1 \tag{40}$$

Again, in the material interpretation, (38) represents the material properties of the cylindric concentrator in the original space (r',ϕ',z'). Fig. 4 shows the radial and

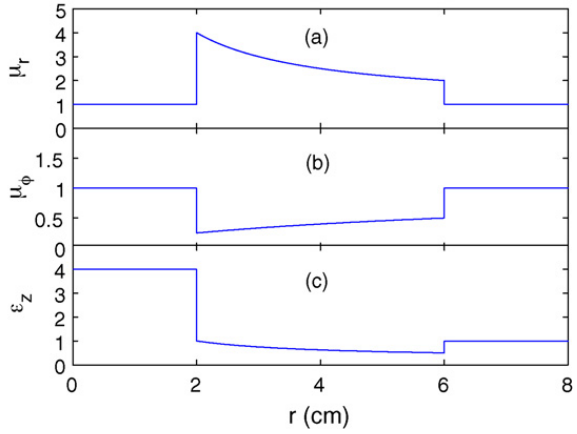

Fig. 4. Radial dependence of the material properties of a cylindric concentrator with an inner radius $R_1 = 2$ cm and an outer radius $R_2 = 6$ cm. (a) radial permeability component μ_r, (b) azimuthal permeability component μ_ϕ, (c) z-component ϵ_z of the permittivity.

azimuthal components $\mu_r := \mu_r^{1'1'}$ and $\mu_\phi := \mu_r^{2'2'}$ and the z-component $\epsilon_z := \epsilon_r^{3'3'}$ in dependence on the radial position within the concentrator, assuming an interaction with an electromagnetic wave with a polarization of the electric field parallel to the z-direction. The experimental implementation of such a material requires independent control of the local values of all three parameters. The metamaterial design and fabrication is part of current research.

3. Simulation results and discussion

For the full wave electromagnetic simulations a two-dimensional finite-element solver of the Comsol Multiphysics software package was used. The computational domain and its boundaries are shown in Fig. 5. A transverse-electric (TE) plane-wave was excited by a current sheet. The computational domain was terminated by perfectly matched layers (PMLs). The current density distribution was chosen to exponentially decrease towards the borders of the sheet in the y-direction to prevent interactions with the PMLs. The calculations did not include absorption in the object. The finite-element solver required all physical quantities to be described in cartesian coordinates. For all simulations, a stationary solver was used. The solver allowed to conveniently implement the functional dependence of the permittivity and permeability tensors of the simulated material into the model and thus to accurately describe and predict the electromagnetic behavior of the designed medium.

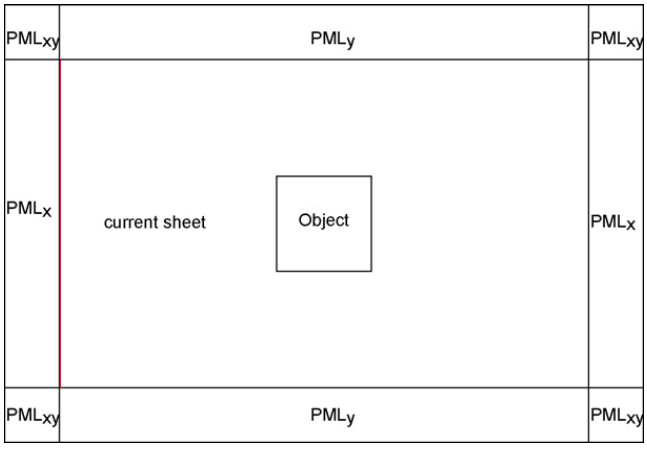

Fig. 5. Computational domain terminated by perfectly matched layers with functionality in the x-, y- and x–y-direction. The TE plane wave is excited by a current sheet.

3.1. Square cloak

Fig. 6 shows the results of the two-dimensional full-wave simulations of a square-shaped cloak. The inner square of the cloak is filled with a perfectly electrically conducting material. The color map depicts the spatial distribution of the real part of the transverse-electric phasor oriented along the z-direction. In addition, the direction of the power flow is indicated by the grey lines. The frequency of the TE wave is 8.5 GHz. The sidelengths of the inner and outer square of the cloak are 6 cm and 12 cm, respectively. In Fig. 6a, the phase fronts of the impinging wave are parallely aligned to one of the sides of the cloak. As can be seen, the wave is smoothly bent around the cloaked area and the phase fronts are completely restored when the wave exits the cloak material. The inhomogeneity and the anisotropy of the cloak medium are evident as the direction of the power flow and the phase front normal are not parallel and the angle between the directions changes locally. In Fig. 6b, the cloak is rotated by an angle of $\pi/8$ with respect to the phase fronts of the incoming wave. In this configuration, the phase fronts are no longer parallel to any side of the square cloak. As before, the phase fronts are completely restored after propagation through the cloak material and the inner square is not sensed by the wave. In both cases, the wave impedances of the cloak medium and free space are exactly matched and the device is therefore reflectionless.

The square-shaped cloak is an example of a cloak with reduced symmetry in comparison to a cylindric cloak. In addition, the square cloak possesses sharp corners. The simulations clearly show, that the transformation-optical cloak design is not restricted by cylindric symmetry requirements. In principle, cloaks of arbitrary shape can be designed by use of the transformation-optical approach.

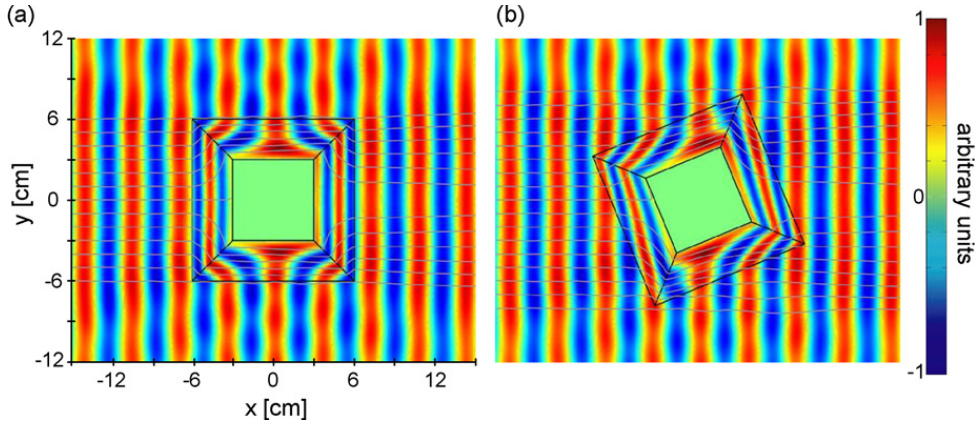

Fig. 6. Electric field distribution in the interior and exterior region of the square cloak. The direction of the power flow is in the positive x-direction. The wave is smoothly bent around the corners of the square cloak. (a) Phase fronts parallel to one side of the cloak and (b) cloak rotated by $\pi/8$ with respect to the phase fronts of the incoming wave.

3.2. Concentrator

In Section 2.2, the material properties of a concentrator were described in a cylindrical coordinate system. In cartesian coordinates, the relative permittivity and permeability tensors can be obtained from (38) by use of the general transformation

$$\xi^{i'j'} = \begin{pmatrix} \frac{1}{r^2}\left(\xi^{11}x_1^2 + \xi^{22}x_2^2\right) & \left(\xi^{11} - \xi^{22}\right)\frac{x_1x_2}{r^2} & 0 \\ \left(\xi^{11} - \xi^{22}\right)\frac{x_1x_2}{r^2} & \frac{1}{r^2}\left(\xi^{22}x_1^2 + \xi^{11}x_2^2\right) & 0 \\ 0 & 0 & \xi^{33} \end{pmatrix} \tag{41}$$

with $\xi = \epsilon_r,\ \mu_r$. The variables ϵ_r and μ_r as functions of the space variables $(x := x_1, y := x_2, z := x_3)$ are then directly assigned to the concentrator domains.

Fig. 7a displays the real part of the phasor of the electric field for a z-polarized TE wave. The grey lines represent the direction of the power flow. The free-space frequency of the TE wave is 8.5 GHz. The outer radius of the concentrator is $R_3 = 6$ cm. As can be seen, the fraction of the plane-wave extending in the y-direction from $-R_2 = -4$ cm to $R_2 = 4$ cm is completely focussed by the concentrator into the region with radius $R_1 = 2$ cm. Additionally, the fields within the intervals $[-R_3, -R_2)$ and $(R_2, R_3]$ in the y-direction are focussed to an area with a radius lying in the interval $(R_1, R_3]$.

Fig. 7b illustrates the normalized intensity distribution of the TE wave. It is obvious, that the field intensities are strongly enhanced in the inner region of radius R_1 within the concentrator material. The intensity enhancement factor for the chosen structure, computed as the ratio between the maximal values of the field intensities outside the circular region with radius R_3 and inside the concentrator region with radius R_1, is 2. Significantly stronger enhancements can be achieved by increasing the ratio R_2/R_1. As can be seen, the enhancement theoretically diverges to infinity as R_1 goes to zero.

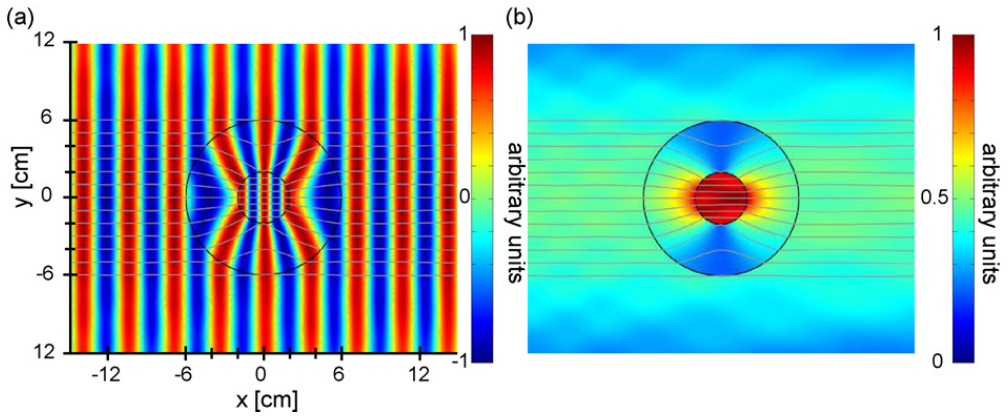

Fig. 7. (a) Electric field distribution in the interior and exterior region of the cylindric concentrator. The direction of the power flow is in the positive x-direction, indicated by the grey lines. (b) Normalized power flow distribution. The power flow is enhanced within the region with radius $R1 = 2$ cm by a factor of 2. Much stronger power flow enhancements can be achieved by increasing the ratio R_2/R_1.

Due to the rotational symmetry around the axis perpendicular to the x–y-plane, the concentrator focusses waves impinging from arbitrary directions. The concentrator is reflectionless due to inherent impedance matching in the transformation-optical design method. Although metamaterials, which are necessary to implement the material properties of a concentrator, inherently suffer from losses, we think, that the concentrator can play an important role in the harnessing of light in solar cells or similar devices, where high field intensities are required.

4. Conclusion

In conclusion, we have presented the material design of a square-shaped cloak and an electromagnetic field concentrator based on form-invariant transformations of Maxwell's equations. The electromagnetic behavior of the devices was simulated by use of a two-dimensional finite element solver. In contrary to previous publications, the simulated cloaking device did not possess a cylinder-symmetry. The proposed electromagnetic field concentrator proved to be well suited for the confinement of electromagnetic energy of waves impinging from arbitrary directions. The two demonstrated optical devices exemplify the strength of the general methodology of form-invariant coordinate transformations of Maxwell's equations for the design of electromagnetic materials with a well-defined functionality. The technique allows to chose from an infinite set of allowed transformations and thus provides a powerful tool for the conception of optical elements with previously unachievable electromagnetic behavior.

Acknowledgement

D. Schurig wishes to acknowledge support from the IC Postdoctoral Research Fellowship program.

References

[1] J.B. Pendry, D. Schurig, D.R. Smith, Science 312 (2006) 1780.
[2] D. Schurig, J.J. Mock, B.J. Justice, S.A. Cummer, J.B. Pendry, A.F. Starr, D.R. Smith, Science 314 (2006) 977.
[3] A.F. Kay, IEEE Trans. Antennas Propagat. AP-13 (1965) 188.
[4] W.V.T. Rusch, J. Appel-Hansen, C.A. Klein, R. Mittra, IEEE Trans. Antennas Propagat. AP-24 (1976) 182.
[5] P.-S. Kildal, A.A. Kishk, A. Tengs, IEEE Trans. Antennas Propagat. AP-44 (1996) 1509.
[6] A. Alu, N. Engheta, Phys. Rev. E 72 (2005) 016623.
[7] M. Kerker, J. Opt. Soc. Am. 65 (1975) 376.
[8] A. Greenleaf, Y. Kurylev, M. Lassas, G. Uhlmann, arXiv:math/0611185v3 (2006)
[9] U. Leonhardt, Science 312 (2006) 1777.
[10] G.W. Milton, M. Briane, J.R. Willis, New J. Phys. 8 (2006) 248–267.
[11] G.W. Milton, N.-A.P. Nicorovici, Proc. R. Soc. Lond. A 462 (2006) 1364.
[12] S.A. Cummer, D. Schurig, New J. Phys. 9 (2007) 45.
[13] W. Cai, U.K. Chettiar, A.V. Kildishev, V.M. Shalaev, Nat. Photon. 1 (2007) 224.
[14] Z. Ruan, M. Yan, C.W. Neff, M. Qiu, Phys. Opt. (2007).
[15] H. Chen, C.T. Chan, arXiv:physics/0702050v2 (2007).
[16] D.A.B. Miller, Opt. Expr. 14 (2006) 12457.
[17] B. Wood, J.B. Pendry, J. Phys.: Condens. Matter 19 (2007) 076208.
[18] S.A. Cummer, B.-I. Popa, D. Schurig, D.R. Smith, Phys. Rev. E 74 (2006) 036621.
[19] F. Zolla, S. Guenneau, A. Nicolet, J.B. Pendry, Opt. Lett. 32 (2007) 1069.
[20] D. Schurig, J.B. Pendry, D.R. Smith, Opt. Expr. 14 (2006) 9794.
[21] E.J. Post, Formal Structure of Electromagnetics, Dover Publications, 1997.
[22] J.A. Schouten, Tensor Analysis for Physicists, Clarendon Press, 1951.